



Title	Quench Hardening and Cracking in Electron Beam Weld Metal of Carbon and Low Alloy Hardenable Steels
Author(s)	Arata, Yoshiaki; Matsuda, Fukuhisa; Nakata, Kazuhiro
Citation	Transactions of JWRI. 1972, 1(1), p. 39-51
Version Type	VoR
URL	<a href="https://doi.org/10.18910/8316">https://doi.org/10.18910/8316</a>
rights	
Note	

*The University of Osaka Institutional Knowledge Archive : OUKA*

<https://ir.library.osaka-u.ac.jp/>

The University of Osaka

# Quench Hardening and Cracking in Electron Beam Weld Metal of Carbon and Low Alloy Hardenable Steels<sup>†</sup>

Yoshiaki ARATA\*, Fukuhisa MATSUDA\*\* and Kazuhiro NAKATA\*\*\*

## Abstract

*Using seventeen kinds of hardenable steel of plain carbon, Ni-Cr, Cr-Mo, Ni-Cr-Mo low alloy and partly 13 Cr steels the hardenability was investigated for the electron beam weld metals which were welded with a change in welding parameters and preheating temperature. Then a generalized prediction equation for the hardness of electron beam weld metal was established using the concepts of the carbon equivalent and the cooling time from 800°C to 500°C. Hereafter the hardness of the weld metal can be estimated in advance when the chemical compositions of steel, the welding parameters, the preheating temperature and the penetration depth are given.*

*Moreover the occurrence of four kinds of crack in weld metal, Horizontal Crack, Vertical Crack (I), Vertical Crack (II) and Cold Shut, was macro-and microscopically investigated. As a result the Vertical Crack (II) is only related to weld metal hardening, while the other cracks occur during solidification of weld metal.*

## 1. Introduction

One of the most advantageous features in electron beam welds results in a deep, narrow and parallel-sided fusion zone in spite of low weld heat input.

The low weld heat input to the parent metal in electron beam welding confines the metallurgical changes to a narrow band on either side of the weld centerline in comparison with any other conventional arc welding. However, as electron beam welding is a fusion welding process, the same metallurgical effects as in any other fusion process occur in both the fusion and the heat-affected zones, although the associated heating and cooling rates and temperature gradients are much higher in the case of electron beam welding. Therefore electron beam welds are also subject to the similar metallurgical basic difficulties as any other fusion welding process including cracking, porosity, lack of fusion, hardening and softening and so forth. With steels which are hardenable by a phase change on cooling, structures which are harder than would be obtained with other fusion processes are produced. This usually due to the formation of a martensitic structure. The hardness reached depends mainly on the carbon and other some alloying elements.

The hardness of the conventional arc weld deposit can be controlled since filler additions are made in the welding process. However, with electron beam welding, it is usual to melt only the parent metal although some investigations have been undertaken to assess

the value of filler materials in reducing peak hardening.

In certain materials, hardened welds will be prone to quench cracking under conditions of high restraint, necessitating the use of preweld and/or postweld heat treatment.

Moreover the high hardness of the weld area are generally undesirable because they constitute a sudden change in material properties in the weld zone.

Therefore with electron beam welding of hardenable steels it is very important to investigate the hardness of weld metal with or without preheating under various welding conditions. Furthermore the relation between hardening and quench cracking in the weld metal is also very important for practical purposes.

Unfortunately few investigation, however, has been done<sup>1)-2)</sup> only for particular steels within authors' knowledge.

In this report, therefore, authors have treated hardening and cracking in electron beam weld metals of various carbon and low alloy hardenable steels.

Firstly, using seventeen kinds of hardenable steel, the maximum hardness in each weld metal with three electron beam welding conditions with or without preheating has been investigated. Then an experimental equation which can estimate the maximum hardness in these electron beam weld metals in advance of welding has been established. Finally the occurrences of weld crackings which are often found in weld metal have been discussed in relation to welding conditions.

<sup>†</sup> Received on May 31, 1972

\* Professor

\*\* Associate Professor

\*\*\* Graduate Student

## 2. Experimental Procedure

### 2.1 Materials used

Commercial five carbon steels, the carbon content of which varies from 0.18 to 0.53 %, four nickel-chromium low alloy steels, two chromium-molybdenum low alloy steels, four nickel-chromium-molybdenum low alloy steels and additionally two 13 % chromium alloy steels are used in this experiment. The chemical compositions of these steels used are shown in Table 1.

These steels were prepared as a rod shape of 50 to 55 mm in diameter and 500 mm in length for electron beam welding purpose.

### 2.2 Welding conditions

For electron beam welding 30 kV—500 mA (maximum 15 kW) type machine was used. A bead-on-plate welding was done longitudinally along the side of each rod under each welding condition.

Three welding conditions [A], [B] and [C] have been principally chosen after the preliminary tests. The welding parameters in [A], [B] and [C] are shown in Fig. 1.

The penetration depth in these three welding conditions was given about 5, 10 and 20 mm, respectively.

Moreover preheating conditions of 150 and 300°C other than room temperature (about 20°C) have been

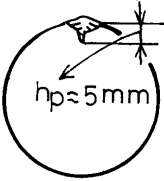
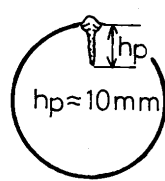
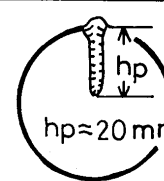
Welding condition		
[A]	[B]	[C]
		
30 kV 90 mA 500 mm/min	30 kV 190~200 mA 500 mm/min	30 kV 370~380 mA 500 mm/min

Fig. 1. Welding Conditions used in This Experiment.

adopted for each welding condition.

### 2.3 Hardness measurement and microscopic observation

The hardness was measured with Vickers hardness tester with 10 kg load as shown in Fig. 2 (a) for weld metal and in Fig. 2 (b) for welded joint, and then the hardness of weld metal was defined on an average of the values of three points.

For microscopic observation the solutions of alcohol saturated with picric acid and alcohol saturated with picric acid + (1 g/100 g) wetting agent + 0.5 % CuCl<sub>2</sub> + 5 % nital were utilized to reveal the primary

Table 1. Chemical Compositions (wt %) of Specimen used

Material	JIS* SPEC. of material	Chemical composition (wt %)								
		C	Mn	Si	Ni	Cr	Mo	S	P	Cu
Carbon steel	S15C	0.18	0.45	0.23	0.01	0.01	—	0.021	0.009	0.02
	S25C	0.24	0.45	0.24	0.02	0.01	—	0.024	0.007	0.03
	S38C	0.39	0.80	0.29	0.02	0.14	—	0.018	0.022	0.05
	S48C	0.50	0.77	0.26	0.02	0.13	—	0.021	0.017	0.03
	S53C	0.53	0.81	0.28	0.01	0.01	—	0.018	0.014	0.02
Ni-Cr low alloy steel	SNC2	0.31	0.48	0.26	2.68	0.80	—	0.014	0.019	—
	SNC3	0.36	0.52	0.26	3.09	0.69	—	0.026	0.020	0.13
	SNC21	0.13	0.48	0.30	2.19	0.37	—	0.007	0.011	—
	SNC22	0.12	0.48	0.26	3.10	0.88	—	0.023	0.015	0.15
Cr-Mo low alloy steel	SCM4	0.39	0.73	0.29	0.03	1.00	0.18	0.014	0.020	0.02
	SCM21	0.18	0.67	0.30	0.10	1.03	0.17	0.014	0.015	0.17
Ni-Cr-Mo low alloy steel	SNM2	0.23	0.51	0.24	3.15	1.13	0.18	0.017	0.017	0.10
	SNM5	0.28	0.57	0.31	2.58	2.66	0.51	0.010	0.020	—
	SNM8	0.41	0.74	0.26	1.70	0.71	0.17	0.010	0.017	0.13
	SNM9	0.46	0.73	0.26	1.71	0.80	0.21	0.011	0.017	—
13Cr steel	SUS50	0.09	0.78	0.29	—	11.90	—	0.009	0.024	—
	SUS53	0.32	0.55	0.48	—	13.30	—	0.006	0.025	—

\* JIS: Japan Industrial Standard

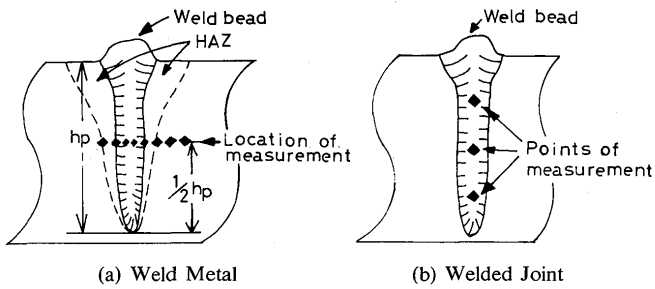


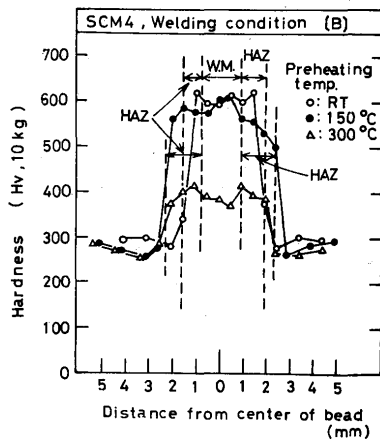
Fig. 2. Illustrations for Hardness Measurements.

dendritic structures of solidification and the prior austenitic grain boundaries, respectively.

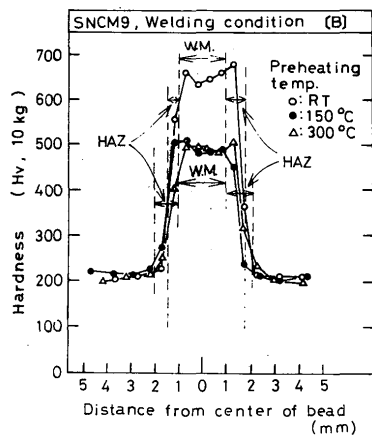
### 3. Consideration on Weld Hardenability

#### 3.1 Hardness in weld metal

As described in the previous report<sup>1)</sup>, the maximum hardness in electron beam welded joint without filler metal is usually seen in the weld metal where the cooling rate is the maximum. Typical examples of the hardness distribution for welded joints of some steels used in this experiment are shown in Fig. 3 (a) and (b).



(a) SCM (Cr-Mo steel)

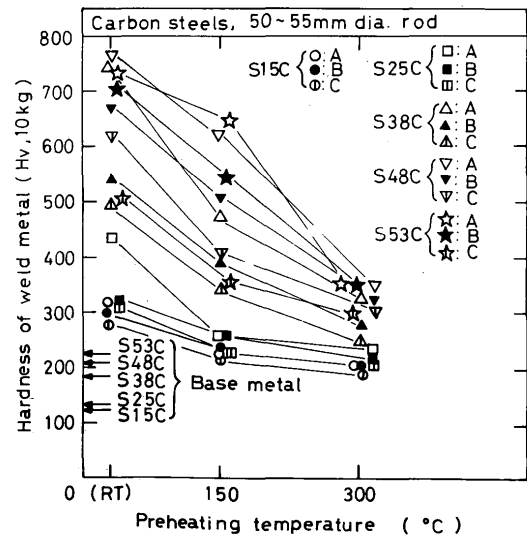


(b) SNCM9 (Ni-Cr-Mo steel)

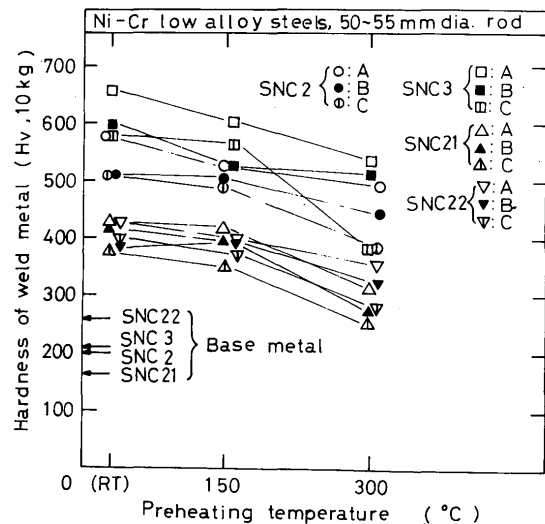
Fig. 3. Hardness Distribution in Cross-section of Welded Joint.

The heat-affected zone as well as the weld metal shows the maximum hardness in electron beam welds of hardenable steels. The higher the preheating temperature, the softer the hardness in the weld metal and the wider the heat-affected zone in general.

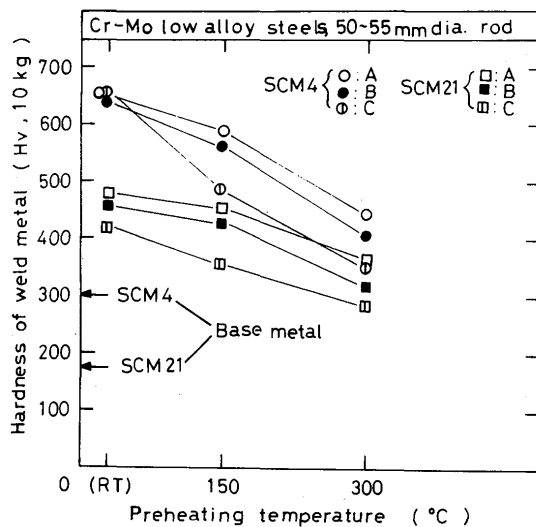
Under the welding conditions of [A], [B] and [C] the relations between the hardness of weld metal and the preheating temperature prior to welding have been investigated for all steels used. These results are shown in Fig. 4 (a) through (e). In Fig. 4 (a) for carbon steels, the weld metals of low carbon steels did not harden so much even in no-preheating condition, but with an increase of carbon the weld metals became harder. Then in the weld metals of S48C and S53C the hardness reached over than 700 when no-preheating welding was applied. However the validity of preheating, which prolongs the cooling time in the weld metal from 800°C to 500°C, is notable for high carbon



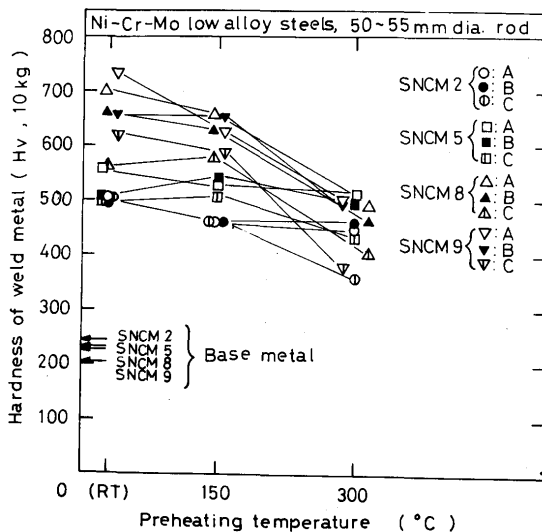
(a) Carbon steel



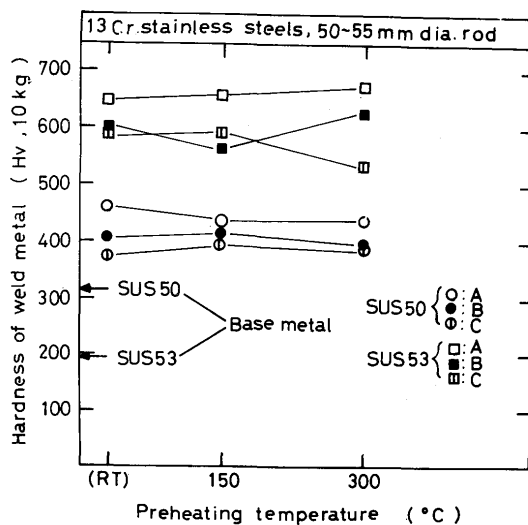
(b) Ni-Cr low alloy steel



(c) Cr-Mo low alloy steel



(d) Ni-Cr-Mo low alloy steel



(e) 13Cr steel

Fig. 4. Relations between Hardness of Weld Metal and Preheating Temperature in [A], [B] and [C] Welding Conditions.

steels because the hardness decreases promptly with an increase of preheating temperature.

In Fig. 4 (b) for Ni-Cr low alloy steels, the hardness of the weld metals are higher in higher carbon Ni-Cr steels such as SNC2 and SNC3 than for lower carbon steels. Moreover the preheating up to 300°C for these Ni-Cr steels is less effective than that for carbon steels.

The results as to Cr-Mo steels are shown in Fig. 4 (c). The difference in the hardness between SCM21 is depended on the difference of carbon content for which the former is about twice more than the latter. The validity of the preheating is recognized a little and the hardness is reduced to about 400 in the weld metals of SCM4 steel which were preheated at 300°C.

The results as to Ni-Cr-Mo steels are shown in Fig. 4 (d). In spite of lower contents of Ni and Cr in SNCM8 and SNCM9 steels, the hardnesses of these no-preheat weld metals are higher than those of SNCM2 and SMCM5 steels because of higher carbon content in the former. However in the 300°C preheat weld metals of the former steels, the hardnesses are reduced noticeably.

In Fig. 4 (e) the results in 13 Cr stainless steels are shown. The weld metals of SUS53 steel which contains higher carbon shows higher hardness than those of SUS50 steel regardless of preheating temperature. Moreover the preheating up to 300°C is invalid for reducing the hardness.

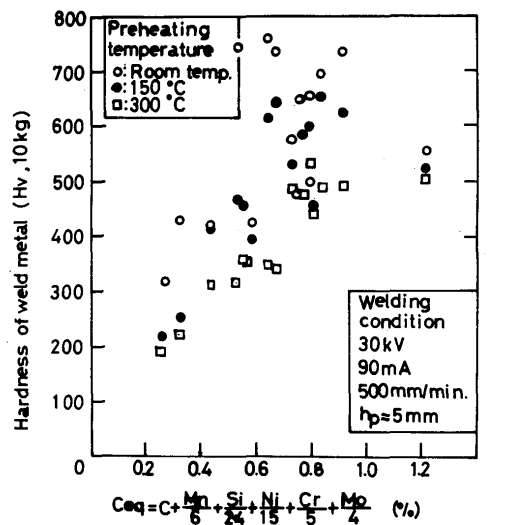
### 3. 2 Arrangement for the hardnesses of the weld metals with the $C_{eq}$ which is widely used for arc welding

The definition of Carbon Equivalent ( $C_{eq}$ ) was widely discussed in the field of arc welding of constructional steels and then various equations for  $C_{eq}$  have already been introduced experimentally with respect to the estimation of the maximum hardness in heat-affected zone of arc welded joint<sup>3)</sup>.

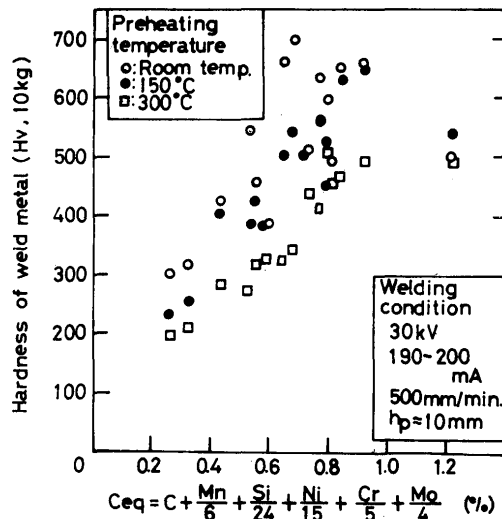
Of the equations the following is widely used for high tensile low alloy steels:

$$C_{eq} = C + Mn/6 + Si/24 + Ni/15 + Cr/5 + Mo/4 \quad (\%) \quad (1)$$

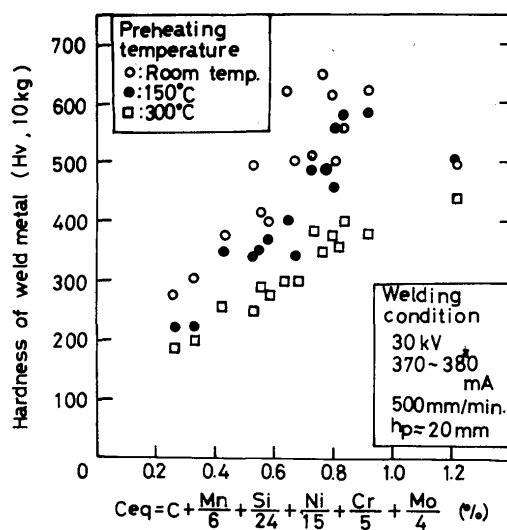
Now authors have tried to obtain the relation between the  $C_{eq}$  in eq. (1) and the hardnesses of electron beam weld metals which were given in Fig. 4. These results are shown in Fig. 5 (a) for [A] welding condition, (b) for [B] and (c) for [C]. In each figure, three kinds of mark show the difference in the preheat temperature. From the results in Fig. 5 there is no close relation between them although some relation can be predicted in [C] condition. It must be considered that there is some limitation for the application



(a) Welding condition [A]



(b) Welding condition [B]



(c) Welding condition [C]

Fig. 5. Relations between Hardness of Weld Metal and Carbon Equivalent for Arc Welding of High Tensile Steels.

of eq. (1) because eq. (1) was obtained from a fixed cooling condition which is given by the defined welding parameters. The cooling condition in the weld metals of the highest heat input of [C] is similar to that in the case of arc welding. Then it seems that hardnesses in [C] welding condition can be fairly put in order with the  $C_{eq}$  for arc welding.

### 3. 3 Prediction for hardness of electron beam weld metal

#### 3. 3. 1 Prediction equation for weld metal hardness to individual welding condition

Using the hardness data obtained, authors have tried to determine new prediction equations for weld metal hardness to individual welding condition by means of the method of least squares. The equations of normal distribution in the method of least squares were computed by means of the iterative process, and FACOM 230-60 is used for this calculation.

In calculation the following two relations were assumed,

$$H_v = a C_{eq} + b \quad (2)$$

$$C_{eq} = [C] + \frac{1}{\alpha_1}[Mn] + \frac{1}{\alpha_2}[Si] + \frac{1}{\alpha_3}[Ni] + \frac{1}{\alpha_4}[Cr] + \frac{1}{\alpha_5}[Mo] \quad (3)$$

where,  $H_v$ : Vickers hardness of weld metal,  $C_{eq}$ : Carbon equivalent (%),  $[C]$ ,  $[Mn]$ ,  $[Si]$ ,  $[Cr]$  and  $[Mo]$ : quantities of carbon, manganese, silicon, nickel, chromium and molybdenum (wt. %), respectively,  $a$ ,  $b$ ,  $1/\alpha_1$ ,  $1/\alpha_2$ ,  $1/\alpha_3$ ,  $1/\alpha_4$  and  $1/\alpha_5$ : constants.

Thus values of " $a$ ", " $b$ ", " $1/\alpha_1$ ", " $1/\alpha_2$ ", " $1/\alpha_3$ ", " $1/\alpha_4$ ", " $1/\alpha_5$ " have been determined for each welding and preheating condition. The results are shown in Table 2 for each condition.

Moreover relations between hardness and the estimated  $C_{eq}$  are shown in Fig. 6 (a), (b) and (c).

From these results there are fairly good relations between them.

Therefore the above each equation of the hardness which was calculated has a validity in the fixed welding and preheating conditions.

Moreover as it is understood from Fig. 6 (a) through (e), all prediction equations for the hardness of the weld metal as well as the  $C_{eq}$  are approximately similar to each other except the inclinations of these straight lines, although there are some differences in detail. It seems, therefore, that all the hardness of electron beam weld metals will be represented in the same  $C_{eq}$  and " $b$ " in eq. (2) with variation of " $a$ ", i. e. the inclination of the straight line. The difference in the inclination of the straight line is caused by the

Table 2. Values of the Coefficients in the Prediction Equations for Weld Metal Hardness.

Welding condition	Preheat temp. (°C)	$\alpha$					a	b	$\sigma$
		Mn	Si	Ni	Cr	Mo			
(A) $\left\{ \begin{array}{l} 30 \text{ kV} \\ 90 \text{ mA} \\ 500 \text{ mm/min} \end{array} \right\}$	RT	2.3	24	34	230	8600	781	88	32
	150	2.4	31	17	23	285	667	38	46
	300	3	18	8.2	5.7	58	387	74	41
(B) $\left\{ \begin{array}{l} 30 \text{ kV} \\ 190 \sim 200 \text{ mA} \\ 500 \text{ mm/min} \end{array} \right\}$	RT	2.1	24	25	70	400	668	70	34
	150	2.2	26	13	14	6.8	541	53	45
	300	4.3	32	8	8.1	7.9	413	64	32
(C) $\left\{ \begin{array}{l} 30 \text{ kV} \\ 370 \sim 380 \text{ mA} \\ 500 \text{ mm/min} \end{array} \right\}$	RT	2.6	22	18	18	610	580	91	50
	150	2.7	31	7.6	12	5.2	444	59	47
	300	2.9	14	9.1	5	9.1	272	85	21

$$C_{eq} = C + \frac{Mn}{\alpha_1} + \frac{Si}{\alpha_2} + \dots, \sigma: \text{Standard deviation of hardness (Hv, 10 kg)}$$

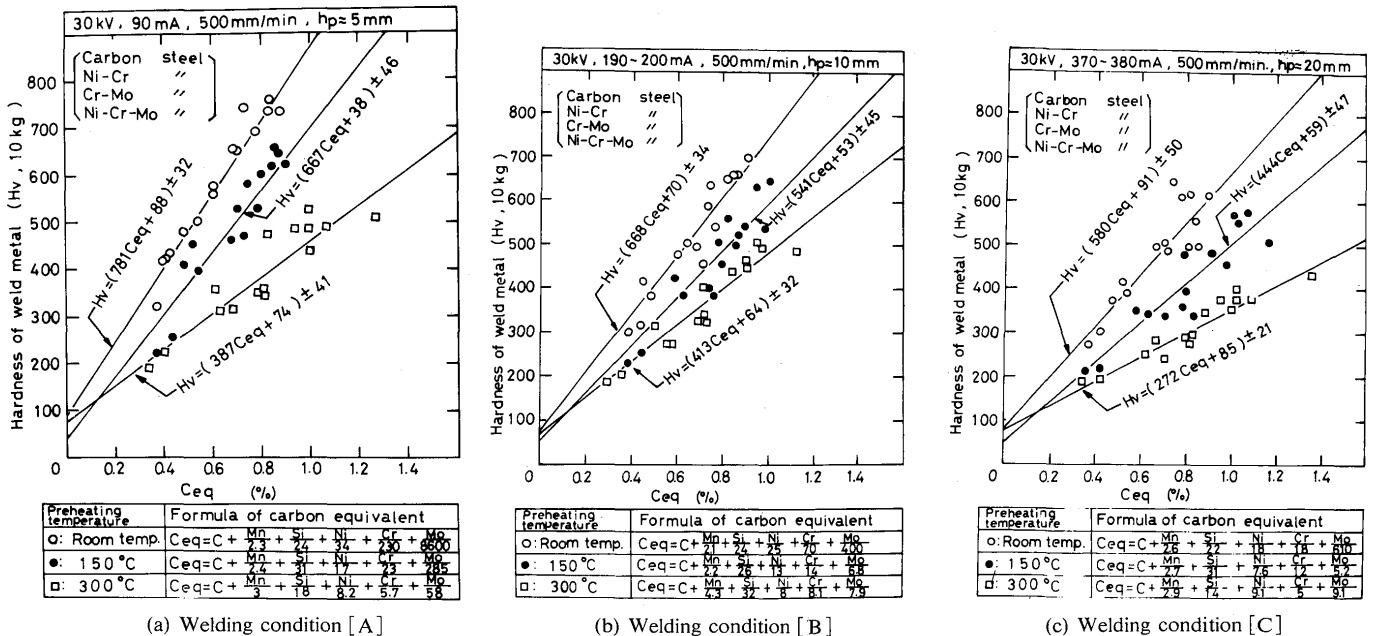


Fig. 6. Relations between Hardness of Weld Metal and Calculated Carbon Equivalent for Individual Welding Condition.

difference in the cooling time passing through the quench temperature range of the steel.

### 3. 3. 2 A Generalized prediction equation for weld metal hardness in electron beam welding

Authors indicated in the above that the weld metal hardness will be estimated in eq. (2) by taking into consideration for the variation in the value of "a" which is related to the cooling time during quenching. Therefore authors have tried to make a new prediction equation for the hardness of all the weld metals that are welded with electron beam welding.

Authors have reported previously on cooling time

of electron beam weld metal from 800°C to 500°C,  $\tau_{800 \rightarrow 500}$ , which decides mainly the hardness of weld metal of hardenable steels<sup>1)</sup>. That is, in case of electron beam welding the cooling time of weld metal from 800°C to 500°C can be easily estimated from the theory of two-dimensional heat flow from a moving line heat source, the depth of which have a length of the bead penetration. Then the cooling time  $\tau_{800 \rightarrow 500}$  was experimentally given by

$$\tau_{800 \rightarrow 500} \div 3.8 \times 10^{-2} \left[ \frac{V \cdot 0.8 I^2}{v \cdot h} \right]^2 \cdot \left[ \frac{1}{(500 - T_0)^2} - \frac{1}{(800 - T_0)^2} \right] \quad (\text{sec}) \quad (4)$$

where, V: accelerating voltage of electrons (kV),

I: emitted current of electron from cathode (mA) (the constant 0.8 means the efficiency of the electron beam from the cathode to the workpiece), v: welding speed (cm/sec),  $h_p$ : penetration of the weld bead (cm),  $T_0$ : initial temperature of the specimen

Moreover authors have established a nomograph eq. (4) as shown in Fig. 7.

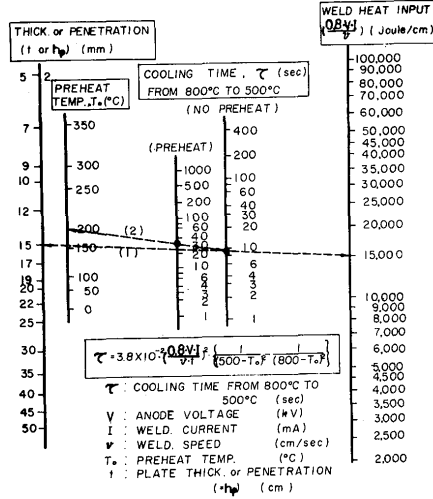


Fig. 7. Nomograph for Estimation of Cooling Time from 800°C to 500°C in Weld Metal

Nextly authors have investigated the relations between the weld metal hardness obtained and the cooling time from 800°C to 500°C which is estimated from eq. (4). These results are shown in Fig. 8 (a) and (b) in logarithmic co-ordinates.

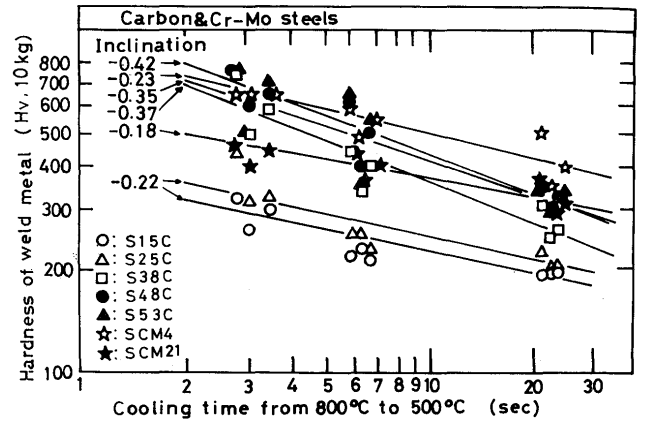
From Fig. 8 authors have learned that each relation can approximately be represented with a straight line within the range of this experiments, while the inclinations of these straight lines respectively show the different value within the range of 0.08 to 0.42.

From the grounds of the above argument authors have assumed the following equations as a new generalized prediction equation for the weld metal hardness, that is

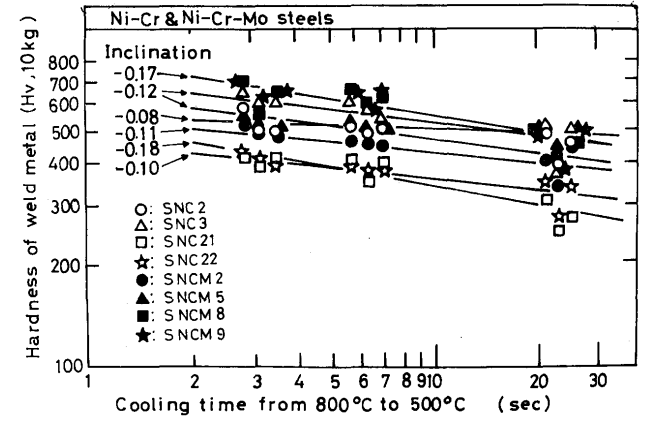
$$H_v = A \left\{ \frac{1}{\tau_{800 \rightarrow 500}^K} \cdot C_{eq} \right\} + B \quad (5)$$

$$C_{eq} = [C] + \frac{1}{\beta_1} [Mn] + \frac{1}{\beta_2} [Si] + \frac{1}{\beta_3} [Ni] + \frac{1}{\beta_4} [Cr] + \frac{1}{\beta_5} [Mo] \quad (6)$$

where, A, B, K,  $\beta_1$ ,  $\beta_2$ ,  $\beta_3$ ,  $\beta_4$ , and  $\beta_5$ : constants,  $\tau_{800 \rightarrow 500}$ : cooling time of weld metal from 800 to 500°C which is estimated by eq. (4) or Fig. 7,  $C_{eq}$ : new carbon equivalent, the equation of which is an identical form in spite of welding condition.



(a) Carbon and Cr-Mo low alloy steels



(b) Ni-Cr and Ni-Cr-Mo low alloy steels

Fig. 8. Relations between Hardness of Weld Metal and Cooling Time from 800°C to 500°C in Weld Metal of Various Steels.

On calculation with the computer, K was firstly assumed for nine different values in the range from 0.16 to 0.24, and subsequently the constants were determined for each K using all the hardness obtained.

The calculations showed that the standard deviation of eq. (5) was the minimum at  $K=0.22$  as shown in Fig. 9.

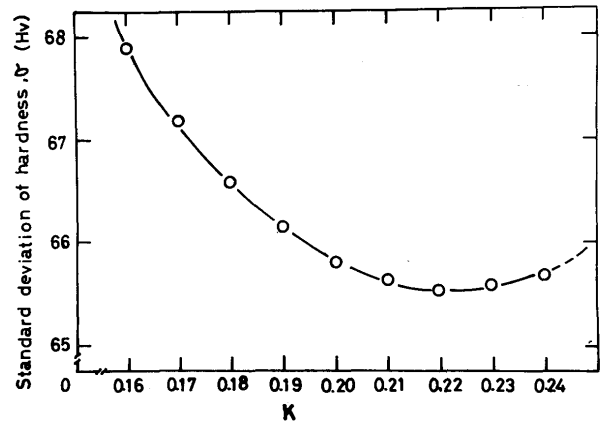


Fig. 9. Relation between K Value and Standard Deviation of Hardness.



Therefore authors have adopted this value of K and then the generalized prediction equation for the weld metal hardness was given by

$$H_v = \left[ \frac{840}{\tau^{0.22}} \cdot C_{eq} + 58 \right] \pm 66 \quad (7)$$

$$C_{eq} = [C] + \frac{[Mn]}{2.4} + \frac{[Si]}{24} + \frac{[Ni]}{14} + \frac{[Cr]}{16} + \frac{[Mo]}{60} \quad (8)$$

where,  $H_v$ : Vickers hardness of weld metal with load of 10 kg,  $\tau$ : cooling time from 800 to 500°C which is estimated by eq. (4) or Fig. 7,  $C_{eq}$ : carbon equivalent, [C], [Mn], [Si], [Ni], [Cr] and [Mo]: wt. % of carbon, manganese, silicon, nickel, chromium and molybdenum.

Note that eq. (7) is reliable on the carbon and the low alloy steels, the chemical compositions of which are within the limits of 0.1 to 0.55 % C, 0.4 to 0.9 % Mn, 0.2 to 0.3 % Si, less 3.5 % Ni, less 3.0 % Cr, less 0.5 % Mo and less 0.2 % Cu.

The experimental relation between the actual hardness of the weld metals and the predicted hardness from eq. (7) is shown in Fig. 10. Most data (about 70 %) are contained within the limits of the standard deviation ( $\pm 66$ ), though some of them deviate from both broken lines.

Moreover, in order to confirm the above relation authors have tried to arrange the actual data of hardness, which were obtained in the electron beam weld metals by several researchers,<sup>1, 2, 4, 5)</sup> with the predicted

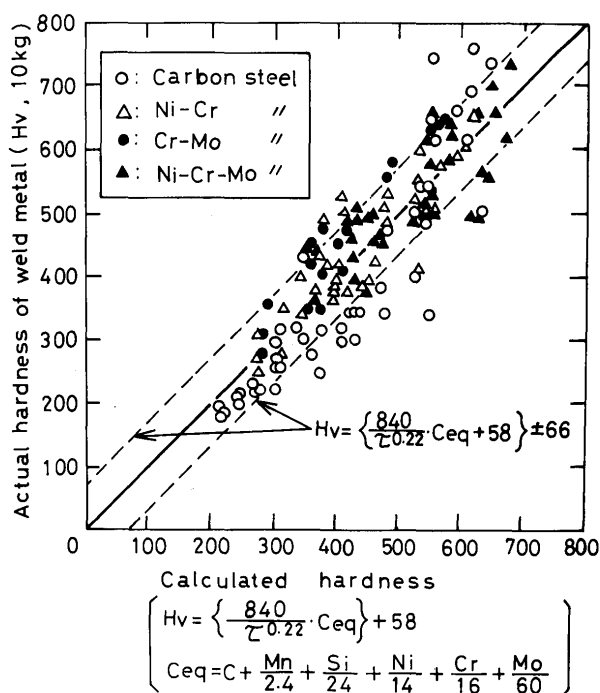


Fig. 10. Comparison of the Actual Hardness with the Calculated Hardness for Electron Beam Weld Metal of Various Steels in This Experiment.

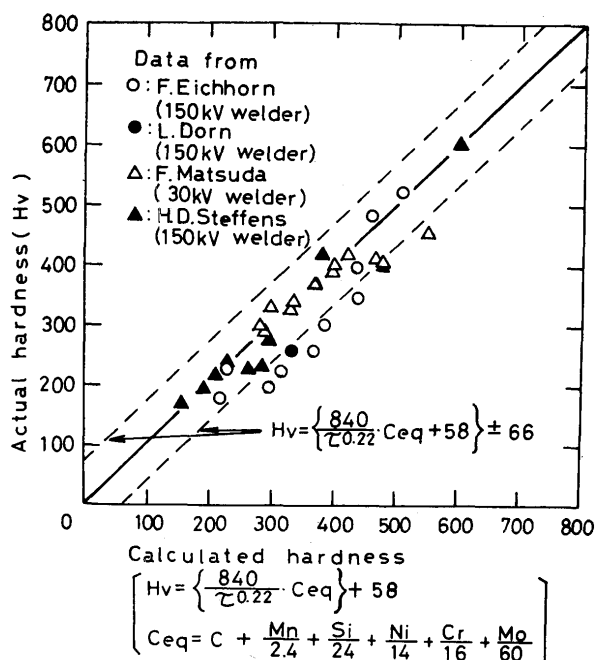


Fig. 11. Comparison of the Actual Hardness of Weld Metals, Which were Measured by Four Researchers, with the Calculated Hardness

hardness by eq. (7) using the cooling time from the welding parameters and the chemical compositions of the steel used. The result is shown in Fig. 11.

These data had been obtained from the different types of welder using some plain carbon, low alloy and high tensile steels.

From a result of Fig. 11 it is considered that equation (7) is fairly valid to predict the hardness of weld metal in electron beam welding of hardenable carbon and low alloy steels.

The hardness of the weld metal, therefore, can be calculated in advance using the welding parameters, preheating temperature, penetration depth predicted and chemical compositions.

The relations between the cooling time of weld metal from 800 to 500°C which is estimated from Fig. 7 and the carbon equivalent in eq. (8) are collectively shown in Fig. 12.

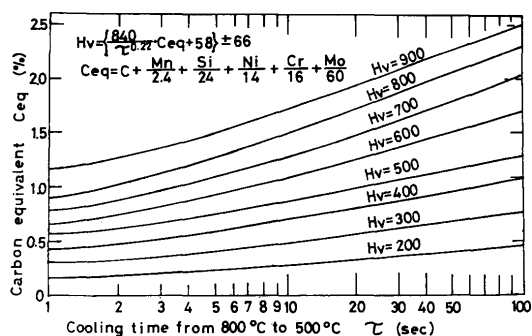


Fig. 12. Estimation Graph for Weld Metal Hardness Which is Determined from Carbon Equivalent and Cooling Time from 800°C to 500°C.

#### 4. Consideration on Weld Metal Cracking

##### 4. 1 Occurrence limits of Weld Cracks

There are various kinds of cracks in electron beam weld metal. These cracks are collectively illustrated in Fig. 13. Of these weld cracks Vertical Crack (II) is

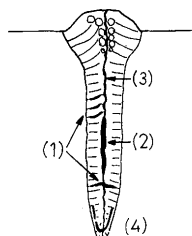


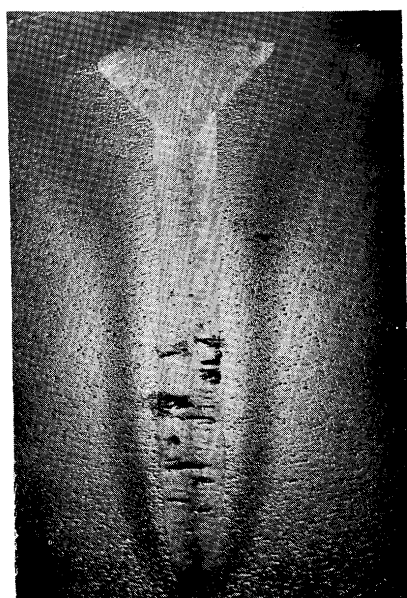
Fig. 13. Schematic Illustration of Various Cracks Which Occur in Electron Beam Weld Metal. (1) Horizontal Crack, (2) Vertical Crack (I), (3) Vertical Crack (II) and (4) Cold Shut.

said to be a cold crack, while the others are said to be hot cracks during solidification.

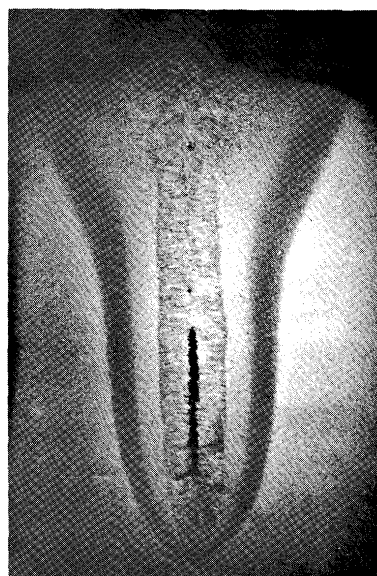
Some typical examples of the weld cracks which were found in this experiment are shown in Fig. 14 (a) through (e).

For all 153 weld beads in this experiment authors have investigated the effects of welding condition including preheating on the occurrence of three kinds of crack. These results are collectively shown in Fig. 15.

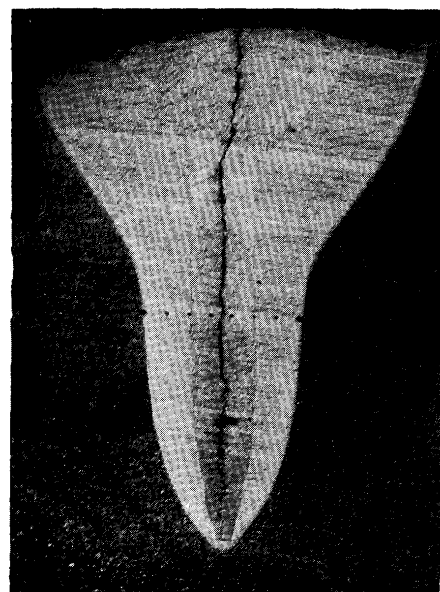
Horizontal Crack occurred in 32 beads (about 20 %), Vertical Crack (I) in 8 (about 5 %) and Vertical Crack (II) in 5 (about 3 %) out of 153 beads. Moreover the Horizontal Crack and the Vertical Crack (I) are abruptly increased in the weld metals with the welding condition [C], the penetration of which shows the deepest in this experiment. On the contrary



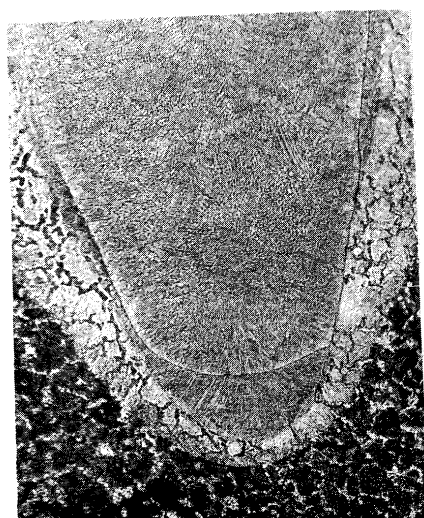
(a) Horizontal Crack (SNC2 steel) ( $\times 2.5$ )



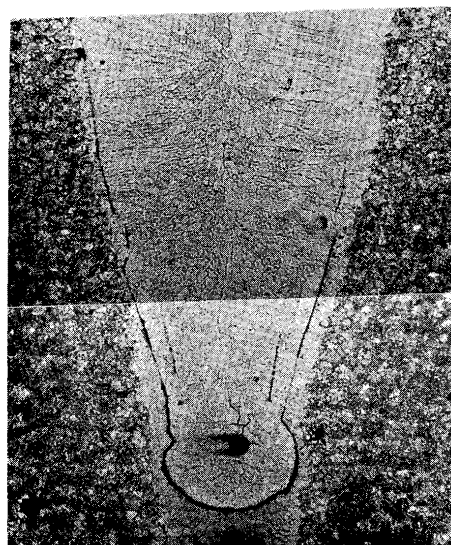
(b) Vertical Crack (I) (SNC2 steel) ( $\times 0.9$ )



(c) Vertical Crack (II) (SCM4 steel) ( $\times 1.0$ )



(d) Cold Shut (S53C steel) ( $\times 100$ )



(e) Cold Shut with Crack (SNC2 steel) ( $\times 42$ )

Fig. 14 Typical Examples of Various Cracks Which Occurred in Weld Metals in This Experiment.

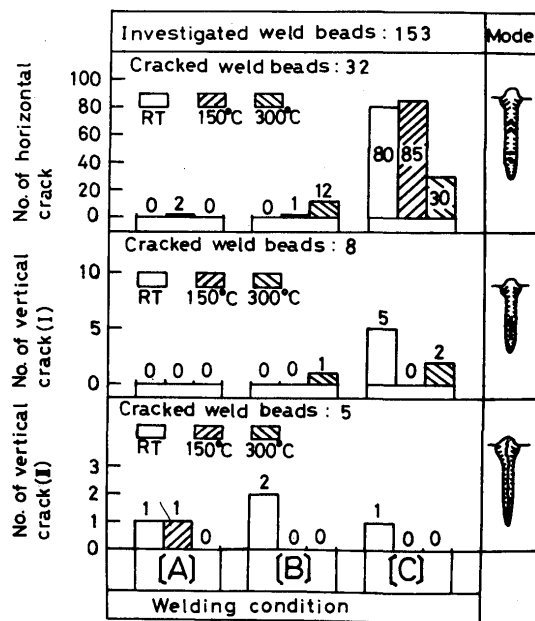


Fig. 15. Relation between Occurrence of Cracks and Welding and Pre-heating Conditions.

the Vertical Cracks (II) are apt to occur in the weld beads without preheating, the cooling rates of which are usually higher.

It is said in the field of arc welding that the harder in the heat-affected zone, the much susceptible for cold cracking. This will also exist in the field of electron beam welding. Therefore authors have investigated for all weld beads the relation between the hardness of the weld metal and the occurrence of weld cracks. The result is shown in Fig. 16. The axes of

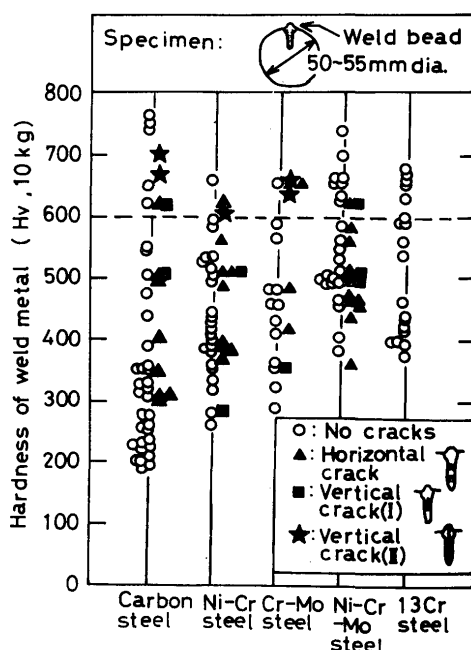


Fig. 16. Relation between Hardness of Weld Metal and Occurrence of Various Cracks.

co-ordinates are the hardness of weld metal and the kinds of steel in which three kinds of crack are shown in three different marks. As a conclusion, the occurrence of the Vertical Crack (II) is only depended on the hardness of weld metal. The limit of the hardness above which the Vertical Crack (II) occurred in the weld metal was placed about 600 in Vickers hardness number. That is to say, the Vertical Crack (II) is much susceptible for electron beam weld metal, the hardness of which exceeds the critical value of about 600 ( $H_v$ ). Of course it is considered that this critical hardness will be lowered when the restraint of the weld joint is increased.

From the above result it seems to authors that the Vertical Crack (II) is a cold crack, while the other two cracks are incorporated into hot cracks.

#### 4. 2 Metallographic observations of weld cracks

##### 4. 2. 1 Horizontal crack

As shown in Fig. 14 (a) the horizontal cracks occur intercolumnar. This is confirmed with Fig. 17 which shows the origin of the crack. This kind of crack, occurs during the final stages of solidification usually because of the low melting point compounds formed by impurities such as sulphur. Examples of the sulphur prints for two welds are shown in Fig. 18 (a) and (b) for SNC2 and SNCM9 steels, respectively.

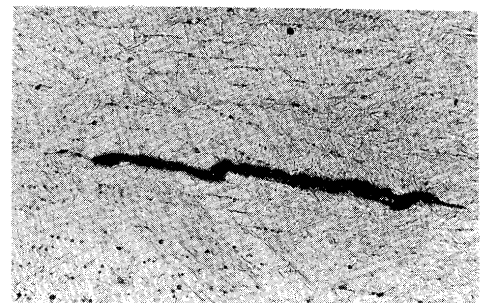
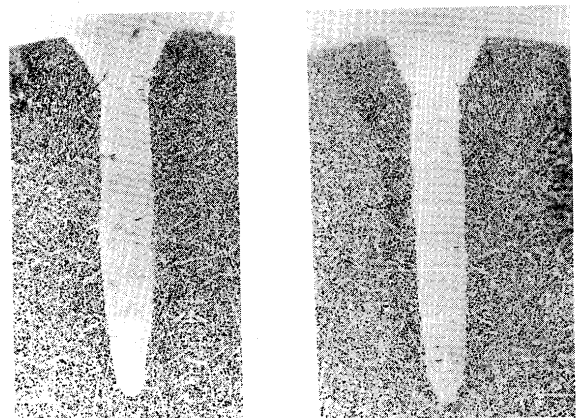


Fig. 17. Horizontal Micro-crack Occurring in Weld Metal of Ni-Cr Steel (SNC3) ( $\times 200$ ).



(a) Ni-Cr steel (SNC2) (b) Ni-Cr-Mo steel (SNCM9)

Fig. 18. Sulphur Print in Cross-section of Welded Joint.

It is clear from both sulphur prints that sulphur is fairly reduced in electron beam weld metal as compared with base metal because of evaporation. However intercolumnar sulphur bands are sporadically seen, and there the Horizontal crack usually occurs.

#### 4. 2. 2 Vertical Crack (I)

Judging from the crack appearance shown in Fig. 14 (b), this kind of crack also occurs during the final stages of solidification where the grain boundaries at the weld centerline have to take large strains. Therefore this is a solidification crack.

#### 4. 2. 3 Vertical Crack (II)

As previously described, this type of crack is closely related to the hardenability of weld metal. In the weld beads over than 600 in Vickers hardness number this was found as shown in Fig. 16.

Microstructural observations of the typical crack are shown in **Fig. 19 (a)** and **(b)** in panoramic fashion. The solidification structure is revealed in Fig. 19 (a) and the austenitic grain boundaries in (b). The enlarged pictures of the crack are shown in **Fig. 20** for Fig. 19 (a) and in **Fig. 21** for Fig. 19 (b). As a result of the microstructural observations it was made clear that the propagation of this crack does not occur along the dendritic boundaries of solidification structure but occur along the grain boundaries of austenitic secondary structure of the weld metal.

Therefore it seems that this kind of crack is a cold crack which occurs in the temperature below  $M_s$  after solidification was completed.

#### 4. 2. 4 Cold Shut

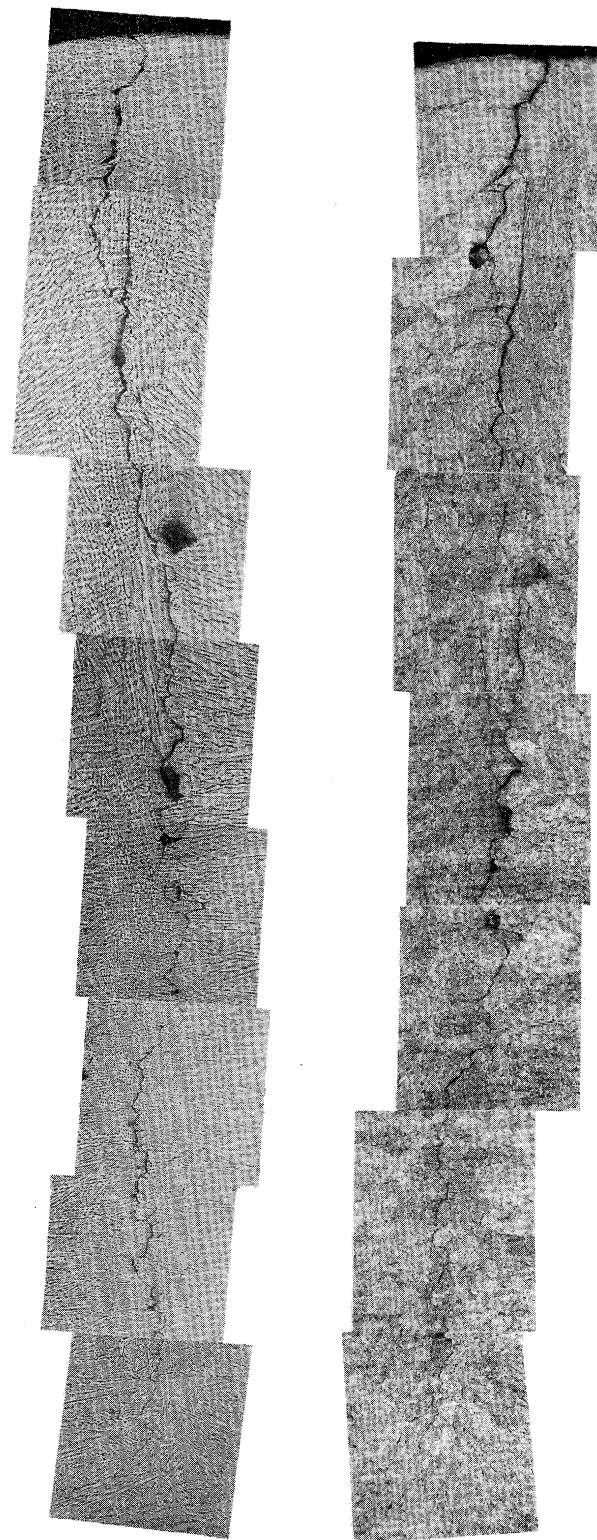
This kind of crack is one of the lack of fusion at or near the tip of penetration as shown Fig. 14 (d) and (e). Examples of the microstructure near the Cold Shut are shown in **Fig. 22 (a)** and **(b)**. The growing directions of the substructures on either side of the Cold Shut are apparently different, therefore these grains will be different in their crystallographic orientations.

The Cold Shut will be caused by the intermittent flow of molten metal pushing backward the electron beam which is illustrated in **Fig. 23**.

### 5. Conclusion

The hardenability and the crack susceptibility in electron beam weld metals of carbon, Ni-Cr, Cr-Mo and Ni-Cr-Mo low alloy and partly 13Cr alloy steels have been investigated. The main conclusions of this investigation are summarized below.

(1) The electron beam weld metals without preheating



(a) Solidification structure

(b) Prior austenitic grain

Fig. 19. Panoramic Pictures of Vertical Crack (II) in Weld Metal of High Carbon Steel (S53C) ( $\times 100$ ).

of high carbon, low alloy and 13Cr steels are so high in hardness that the occurrence of weld cracks or the insufficient ductility in the welded joint are often observed. Therefore preheating and/or post heat treat-

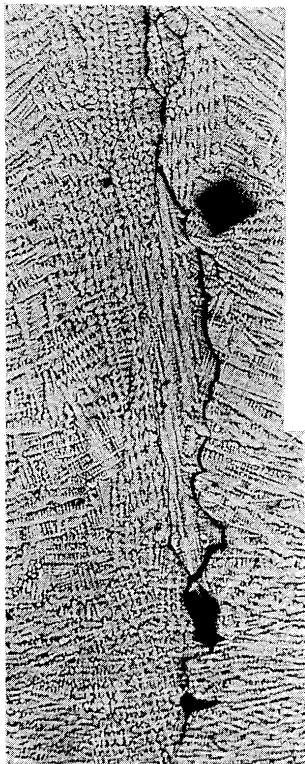


Fig. 20. Microstructure of Cracking Zone in Fig. 19 (a) (Solidification Structure) ( $\times 100$ ).

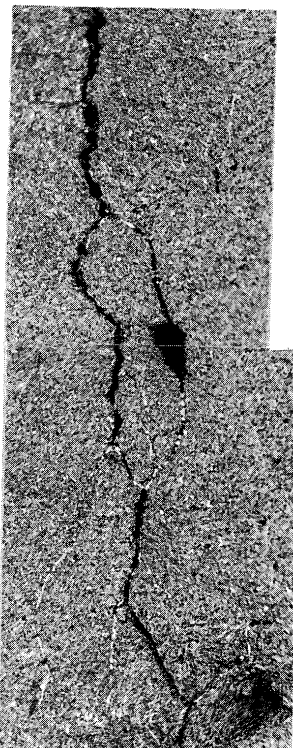
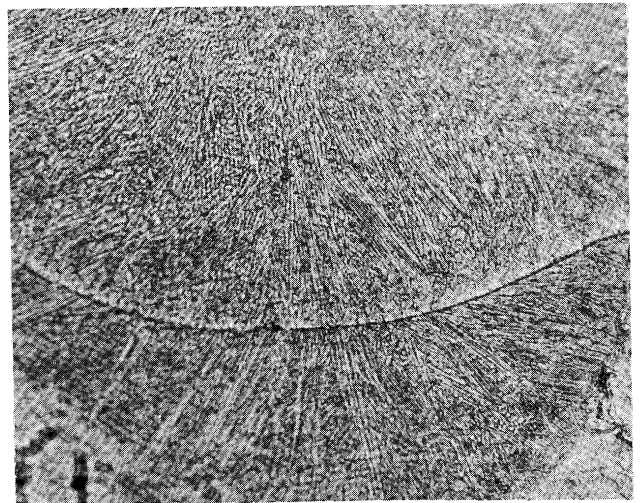
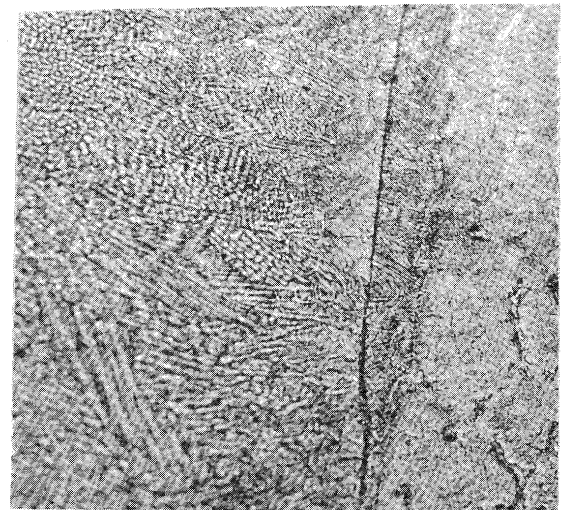


Fig. 21. Microstructure of Cracking Zone in Fig. 19 (b) (Prior Austenitic Grain) ( $\times 200$ ).



(a) Tip of Cold Shut



(b) Side of Cold Shut

Fig. 22. Solidification Microstructures on Both Sides of Cold Shut ( $\times 200$ ).

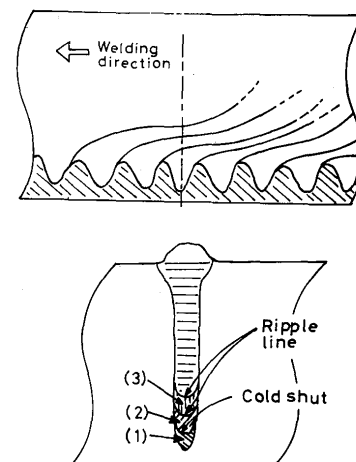


Fig. 23. Schematic Illustration of Cold Shut from Longitudinal and Cross-sections of Welds.



ment are required to obtain the sound welds for electron beam welding of these steels.

(2) As to carbon steel in higher level of carbon, the hardness of the weld metal can be reduced to less than 350 in Vickers hardness number with preheating of 300°C. However the hardness of the weld metals of Ni-Cr, Cr-Mo, Ni-Cr-Mo and 13Cr steels can not be reduced so much with preheating up to 300°C.

(3) It is difficult to predict, in general, the hardness of the electron beam weld metals of various hardenable steels, which are welded with various welding parameters, by using the equation of carbon equivalent which was determined and widely used in the field of arc welding.

(4) Therefore in this investigation, a generalized prediction equation for the weld metal hardness was introduced by introducing a concept of the cooling time of weld metal from 800 to 500°C. This is given by

$$H_V = \left[ \frac{840}{\tau^{0.22}} \cdot C_{eq} + 58 \right] \pm 66$$

where,  $H_V$ : Vichers hardness of the weld metal with 10 kg load,  $\tau$ : cooling time of weld metal from 800°C to 500°C,  $C_{eq}$ : carbon equivalent  $[= C + (1/2.4) Mn + (1/24) Si + (1/14) Ni + (1/16) Cr + (1/60) Mo]$ . However this equation is reliable on the steels whose chemical compositions are within the limits of 0.1 to 0.55 % C, 0.4 to 0.9 % Mn, 0.2 to 0.3 % Si, less 3.5% Ni, less 3.0 % Cr, less 0.5 % Mo and less 0.2 % Cu.

(5) The above prediction equation is also valid for the prediction on the hardness of weld metals which are

welded with the different types of electron beam welder.

(6) Vertical Crack (II) is related to the hardenability of the weld metal, and this crack occurred in the weld metal over than 600 in Vickers hardness number in this experiment.

Moreover this crack propagates through the grain boundaries of the prior austenitic structure, therefore therefore this seems to be a cold crack.

(7) Horizontal Crack, Vertical Crack (I) and Cold Shut seem to occur during solidification of weld metal because the separation occurred in the interdendritic boundaries of the solidification structure.

### Acknowledgments

The authors wish to acknowledge the co-operative support of Japan Electron Optics Industries Co. Ltd.

### References

- 1) F. Matsuda, T. Hashimoto, Y. Arata: "Some Metallurgical Investigations on Electron-beam Welds", *Trans. Japan Welding Society*, **1**, 1, 72-85 (1970).
- 2) F. Eichhorn, D. Schumacher, D. Neef: "Investigations on Electron Beam Welding of Preheated Specimens Made of Unalloyed Steels with a Higher Carbon Content", *IIW Doc. IV-56-71-E*.
- 3) QT Subcommittee IIW IX: "Weldable QT High Strength Steels and Their Applications in Japan", *IIW Doc. IX-673-70*.
- 4) L. Dorn: "Erfahrungen mit dem Electronenstrahlschweissen Allgemeiner Baustähle", *Schw. und Schn.*, **21**, H2 (1969).
- 5) H. D. Steffens, G. H. Sepold: "Recent Development in Electron Beam Welding of Unalloyed Steels", 4th International Conference on Electron and Ion Beam Science and Technology, 1970, 281-291.